Journal of the Chinese Institute of Engineers, Vol. 23, No. 3, pp. 331-338 (2000)

COMPUTATION OF THE FREE SURFACE FLOW AROUND LIFTING AND NON-LIFTING BODIES BY A MIXED POTENTIAL AND VELOCITY BASED BOUNDARY ELEMENT METHOD

Ching-Yeh Hsin[1]* and Shean-Kwang Chou[2]
[1]*Department of Naval Architecture*
National Taiwan Ocean University
Keelung, Taiwan 202, R.O.C.
[2]*United Ship Design and Development Cente*
Keelung, Taiwan 204, R.O.C.

Key Word: boundary element method, free surface, wave making resistance, Kutta condition.

ABSTRACT

The purpose of this paper is to present a mixed potential and velocity based boundary element method to solve wave making resistance problems. In this method, the singularity strengths on a non-lifting body or a lifting body are solved by a potential based boundary element method, and the singularity strengths on the free surface are solved by a velocity based method. The interaction between the body and the free surface is then calculated by an iterative procedure. It is found that a block iterative matrix solver can be used in the solutions, and computational time has thus been dramatically reduced. Computational results are shown for the comparison of the presented method and a source only velocity based method. Calculated results for both non-lifting and lifting bodies are also compared with the experimental data.

I. INTRODUCTION

Solving wave resistance problems by a boundary element method, or a panel method, has been studied for more than thirty years. Hess and Smith (1964) first presented a velocity based boundary element method to calculate the potential flow around an arbitrary three dimensional body, and Dawson (1977) later modified Hess and Smith's method to take the free surface effect into account. In Dawson's method, sources are distributed on both the body surface and the free surface, and strengths of the sources distributed are determined by satisfying the solid body boundary condition on the body, and a linearized free surface boundary condition on the free surface.

For bodies with lifting effects traveling in a free surface, such as a surface piercing hydrofoil, dipoles or vortices have to be distributed on the body surface. Hess (1972) modified his source only method with the inclusion of a constant strength vortex sheet distributed on the body surface, and the vortex strengths are determined by satisfying the Kutta condition. Xia (1986) later applied this modified method to calculate the wave making resistance of a sailing boat. Xu (1991) and Maniar (1990) used Havelock singularities to solve the free surface/lifting surface interaction problems, in which the panels only needed to be distributed on the body surface.

In the present paper, the authors use a different approach by solving the singularity strengths on the

*Correspondence addressee

body surface and on the free surface separately. For solving the body problems, Green's identity formula is adopted, and a potential based boundary element method is used to solve the strengths of perturbation potentials (dipoles) distributed on the body surface by satisfying the solid body boundary condition. For lifting bodies, a vortex sheet (wake) behind the body is introduced, and the Kutta condition has to be satisfied. For the free surface problem, a velocity based method is used to solve the strengths of sources distributed on the free surface, and a linearized free surface boundary condition is imposed on the free surface panel. The interaction between a body and the free surface is considered by including the induced velocities of each other as part of the the inflow, and an iterative procedure is needed to obtain the final solutions.

II. THEORY

Considering a body (a ship or a hydrofoil) traveling with a steady forward speed, U_∞, in the presence of the free surface, and ζ is assumed to be the wave elevation due to the interaction between the body and the free surface. Under the assumption of potential flow, the governing equation is the Laplace equation:

$$\nabla^2\Phi=0 \tag{1}$$

and Φ is the total velocity potential. To satisfy Bernoulli's equation on the free surface $z=\zeta(x,y)$, we have

$$g\zeta+\frac{1}{2}(\Phi_x^2+\Phi_y^2+\Phi_z^2-U_\infty^2)=0 \tag{2}$$

and the kinematics boundary condition gives

$$\Phi_x\zeta_x+\Phi_y\zeta_y-\Phi_z=0 \tag{3}$$

Dawson (1977) linearized the above equations with respect to the "double body" flow, and assumed the total potential Φ to be the sum of the body potential, ϕ_d, and the free surface perturbation potential, ϕ_f.

$$\Phi=\phi_d+\phi_f. \tag{4}$$

The following equation then can be obtained from equations (2), (3), and (4):

$$[(\phi_d)_l^2\Phi_l]_l+g\Phi_z=2(\phi_d)_l^2(\phi_d)_{ll} \tag{5}$$

where l represents the derivatives of the potentials along a streamline on the plane of $z=0$. The boundary condition on the wetted body surface is the solid body boundary condition:

$$\Phi_n=0, \tag{6}$$

where Φ_n is the normal derivative of the total potential.

The above method has been widely applied to solve wave resistance problems, in which sources are distributed on both the body surface and the free surface. Detailed derivation can be seen from Kim (1981), Lu (1994) or other related documents. The lifting effect had not been considered until Xia (1986) applied a modified velocity-based boundary element method to calculate the wave making resistance of a sailing boat. Xia adopted the method modified by Hess (1972), and kept the original structure of Dawson's method. However, the final formulation was very complicated due to the consideration of the lifting effect, and an iterative procedure was necessary to satisfy the Kutta condition.

In the presented method, we solve the body (ship) problem and the free surface problem separately. Both source and dipole sheets are distributed on the body surface, however, only source sheets are distributed on the free surface. The singularity strengths on the body and on the free surface are solved separately, and the influence on each other is then considered by including the induced velocities as part of the inflow velocities.

When solving body problem, Green's theorem is used,

$$2\pi\phi(p)=\iint_{S_B}[\phi(q)\frac{\partial G}{\partial n}-G\frac{\partial\phi}{\partial n}(q)]dS+\int_{S_W}\Delta\phi\frac{\partial G}{\partial n}dS \tag{7}$$

where G is the Green function, $G=\frac{1}{R(p;q)}$, $R(p;q)$ is the distance between points p and q, S_B represents the body surface, and S_W represents the body wake surface. ϕ is the perturbation potential, and can be explained as the dipole strength distributed on the body surface. $\partial\phi/\partial n$ is the source strength, and it is a known term from the solid body boundary condition:

$$\frac{\partial\phi}{\partial n}=-\overline{U}_{in}^{B}\cdot\overline{n} \tag{8}$$

where $\overline{n}$ is the normal vector of the body, $\overline{U}_{in}^{B}$ is the inflow velocity including the induced velocities on the body by the free surface panels, $\overline{u}^*$:

$$\overline{U}_{in}^{B}=\overline{U}_\infty+\overline{u}^* \tag{9}$$

The reason to include the free surface induced velocity in the inflow velocity is to consider the interaction between the body and the free surface, that is, to simulate the free surface effect. However, Green's theorem is still applied to the computational domain composed by the body surface and the boundary at the infinity.

In Eq. (7), $\Delta\phi$ is the dipole strength in the body wake, and it has to be equivalent to the difference of the dipole strengths of panels on the upper and lower surfaces at the trailing edge to satisfy the Kutta condition. This kind of numerical Kutta condition was first used by Morino (1974), and later was applied to a propeller boundary element method by Kerwin *et. al.* (1987). Morino's Kutta condition implies that the vortex strength at the trailing edge is zero, therefore, the pressures on the pressure side and on the suction side are equal at the trailing edge. Notice that $\Delta\phi$ can be coupled into the dipole term in Eq. (7) since it equals to the difference of the dipole strengths at the trailing edge panels.

We begin the solutions of Eqs. (7) and (8) with the "double body" solution, that is, a solution corresponding to the zero Froude number (gravitational force far greater than the inertial force). Therefore, the initial solutions (first iteration) of the Eqs. (7) and (8) are the solutions of the "double body problem", and the influence of the free surface is not included. In the following iterations, the induced velocities on the body by the free surface are included in the inflow velocities, and the solutions of Eqs. (7) and (8) are called the solutions of the "body problem". In each iteration, the term ϕ represents an updated body solution, ϕ_d.

When solving the free surface problem, the derivative of the total potential in the streamline direction thus can be expressed as follows:

$$(\Phi)_l = \overline{U}_{in}^{\infty} \cdot \overline{l} + (\Phi_d)_l + (\Phi_f)_l \tag{10}$$

where $(\phi_d)_l$ can be calculated from Eq. (7), and $(\phi_f)_l = \int_{S_F} \sigma \nabla G dS$, where σ is the source strength on the free surface panel. The inflow term in Eq. (10) is $\overline{U}_{in}^{\infty} \cdot \overline{l} + (\phi_d)_l$, which equals the sum of the inflow velocity and the induced velocities on the free surface panel by the body. Eq. (5) then can be solved to obtain the source strengths on the free surface panels.

In the above scheme, it needs an iterative procedure to include the interaction between the body and the free surface, and the numerical procedure will be discussed in the next section.

III. NUMERICAL IMPLEMENTATIONS

We have introduced the fundamental formulations needed in this method, and we will now describe the numerical procedure.

1. First, we solve the double-body problem by solving the discretized form of Eq. (7) with the boundary condition in Eq. (8). The discretized form of Eq. (7) can be seen form Kerwin *et al.* (1987) or Hsin (1990,1991), and it can be represented by the following linear system:

$$[K_{BB}][\phi_d] = [RHS_B] \tag{11}$$

In Eq. (11), we define the left-hand-side matrix $[K_{BB}]$ as the "body to body" influence coefficients matrix. The right-hand-side matrix $[RHS_B]$ represents the influence of the source with the strength of $-\overline{U}_{in}^{B} \cdot \overline{n}$ (Eq. (8)). We can then obtain the solutions, ϕ_d, by solving the above linear system.

2. We then solve the free surface problem, that is, solve Eq. (5). In Eq. (5), each term can be calculated as follows:
   (a) $(\phi_d)_l$ can be obtained by calculating the induced velocities of the body on the free surface panels,
   (b) $(\Phi)_l$ is replaced by Eq. (10),
   (c) $[(\phi_d)_l^2 \Phi_l]_l$ and $(\phi_d)_{ll}$ can be obtained by using a finite difference method to $(\phi_d)_l^2 \Phi_l$ and $(\phi_d)_l$.
   A linear system thus can be set up from Eq. (5) with the unknowns, ϕ_f,

$$[K_{FF}][\phi_f] = [RHS_F] \tag{12}$$

In Eq. (12), we define the left-hand-side matrix $[K_{FF}]$ as the "free surface to free surface" influence coefficients matrix. The source strengths of free surface panels, ϕ_f, thus can be calculated.

3. Calculate the induced velocities of the free surface panels to the body panels. The inflow velocity to the body is updated by including the free surface induced velocities as in Eq. (9), and the source strength distributed on the body surface is thus updated. The singularity strengths on the body can be solved again by solving Eq. (7), or, step 1. However, the "body problem" instead of the "double body problem" in the first iteration is solved.
4. We can then repeat step 2 by using the updated body problem solutions.

The whole procedure is repeated until solutions are converged.

To further explain the presented method, let's go back to Dawson's method first. In Dawson's method, the matrix system can be grouped as follows:

$$\begin{bmatrix} K_{BB}^{D} & K_{FB}^{D} \\ K_{BF}^{D} & K_{FF}^{D} \end{bmatrix} \begin{bmatrix} \sigma_B \\ \sigma_F \end{bmatrix} = [RHS] \tag{13}$$

where K_{BB}^{D} is the "body to body" influence coefficients matrix, K_{FB}^{D} is the "free surface to body" influence coefficients matrix, K_{BF}^{D} is the "body to free surface" influence coefficients matrix, and K_{FF}^{D} is the "free surface to free surface" influence coefficients matrix. σ_B and σ_F are the source strengths distributed on both the body surface and free surface. By comparing Eq. (11) and (12) with Eq. (13), one can

see that although the influence coefficients are different, the presented method in some sense decomposes the matrix system of Dawson's method into two systems (body problem and free surface problem). That is, only the two diagonal matrices in Eq. (13) are solved.

It is found that an iterative matrix solver can be used to solve both the body and free surface problems, and this is not possible when solving Eq. (13) in Dawson's method. Therefore, less computational time is needed by using the presented method. This must be because a mixed boundary element method is used and the "body problem" and the "free surface problem" are solved separately. If N_B is the number of panels distributed on the body surface, and N_F is the number of panels distributed on the free surface, then the time to calculate the influence coefficients in both methods are equal and proportional to $(N_F+N_B)^2$. The time to solve the matrix system in Dawson's method is proportional to $2/3(N_F+N_B)^3$ by using the LU factorization method. On the other hand, the time to solve the matrix system in the presented method is proportional to $k_B(N_B)^2+k_F(N_F)^2$ (k_B and k_F are number of iterations) using an iterative method when solving the "double body problem" and "free surface problem", and is proportional to $(N_B)^2+(N_F)^2$ when solving the "body problem" and "free surface problem" since only back substitution is needed. In our experience, k_F and k_B are both around 20, and the total number of iterations needed in solving the body problem is less than 5. Overall, the computational time used in solving the matrix system in the presented method is around $25\times((N_B)^2+(N_F)^2)$. For a typical case, N_B is around 1000, and N_F is around 2500, then the time to solve the matrix system in the presented method is only 0.63% of that in Dawson's method. Since the computational time in solving the matrix system in a boundary element method is usually one half of the total computation time, the computational time of presented method is far less than that of Dawson's method.

Because the interaction between the body and the free surface is carried out by the concept of "inflow" here, a body with multiple parts can also be computed by the presented method. The fundamental philosophy is still the same, however, there are two different ways to obtain the body solution. One way is to solve all the "body parts" together just as described above. The other way is to obtain the solutions of each "body part", and the interaction between parts is carried out by the "inflow" concept. For example, when calculating the free surface around a catamaran, although both approaches can be used, the first approach may be easier since two body parts are symmetrical. However, when investigating the interaction between the propeller and the ship hull, the latter approach may be more appropriate.

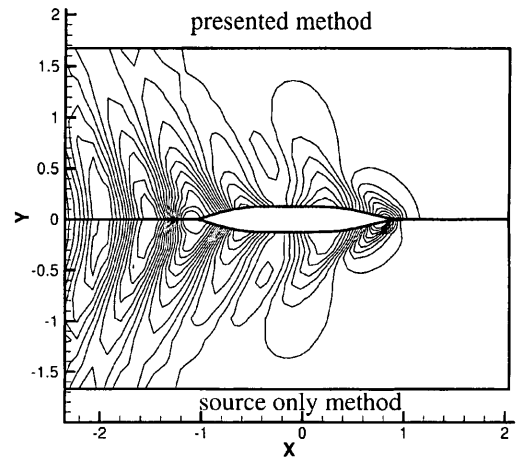

Fig. 1 Comparison of the calculated wave pattern at Froude number 0.28 between the presented method and a source only, velocity based method

IV. NUMERICAL VALIDATIONS

In order to validate the presented method, we will demonstrate several numerical examples here, and these calculations include both the flow around non-lifting bodies and the flow around lifting bodies. The computational results will be used for the following purposes:

- the comparison between the presented method and a source only method for both the lifting and non-lifting bodies;
- the effect of the Kutta condition for the calculation of flow around a lifting body;
- the comparison between the numerical results and the experimental data.

1. Non-Lifting Bodies in the Free Surface

We have first tested the presented method by computing the flow around a non-lifting body, and the case selected is the classical Series 60 ship hull with C_B=0.6. We have calculated the flow around this ship hull at several different Froude numbers to obtain the wave profile and the wave resistance. The Froude number here is defined as $F_n=\frac{U_\infty}{\sqrt{gL}}$, where L is the ship length. The computational results have been first compared with the computational results of a source-only, velocity based, Dawson's type code (Lu and Chou, 1994). Fig. 1 shows the comparison of the calculated wave pattern at Froude number 0.28 between the presented method and the source only velocity based method, and the results from two methods agree with each other pretty well. Note that both methods use exactly the same panel arrangements in the computations.

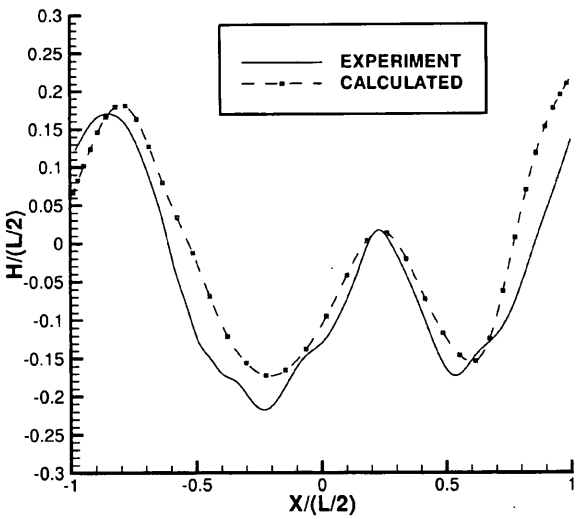

Fig. 2 Comparison of the wave height at Froude number 0.28 between the computational results and the measured values (bow is at -1.0)

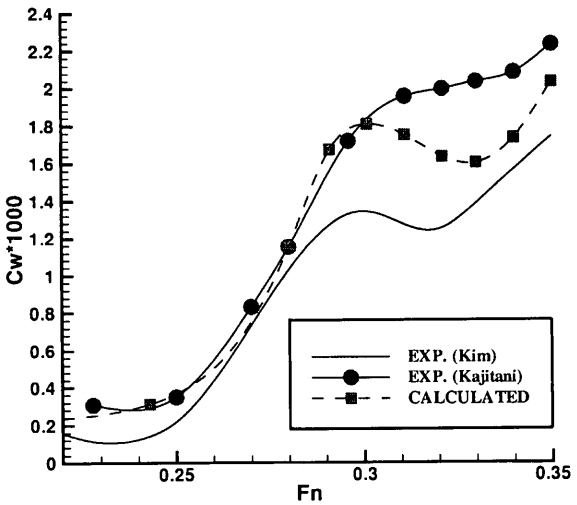

Fig. 3 Comparison of the wave the resistance coefficients, C_W, between the computational results and the experimental data. C_W is defined as $\frac{R_W}{1/2\rho V_s^2 S}$

We then compare the computational results with the experimental data. Fig. 2 shows the comparison of the wave height at Froude number 0.28 between the computational results and the measured data by Kim and Jenkins (1981). In this figure, L is the ship length, and the ship bow and stern are located at x= −1.0 and x=+1.0 respectively. Fig. 3 shows the comparison of the wave resistance coefficients, C_W, between the computational results and the experimental data at different Froude numbers. In this comparison, two different sets of experimental data are used, one is obtained by Kim and Jenkins (1981) and the other one is by Kajitani (1987). Here, C_W is defined as $\frac{R_W}{1/2\rho V_s^2 S}$, where S is the wetted surface area of the ship hull, and V_s is the ship speed. In both figures, the comparisons between the computational results and experimental data are reasonable. In Fig. 3, one can see that the computational results show the same trend with two different experiment data. Although the computational results are consistently higher than the experimental data by Kim and Jenkins, they are very close to Kajitani's data for Froude numbers lower than 0.3. The larger discrepancies for Froude numbers higher than 0.3 are due to the linearization of the free surface boundary conditions used in the presented method.

2. Lifting Bodies in the Free Surface

In order to validate the computations of free surface flow around lifting bodies by using the presented method, the calculations of two surface piercing hydrofoils are demonstrated here. These two hydrofoils are actually the same hydrofoil with different immersed lengths. The experiments have been conducted at David Taylor Model Basin, and forces on the hydrofoils have been measured (Beaver, 1991) at different Froude numbers and different yaw angles (angles of attack). The tested hydrofoil has a NACA63A section with 9% thickness to chord ratio. The chord length is 425.45 mm, and the spans underwater are 1447.8 mm for the "full span" case (the aspect ratio is 3.4), and 762 mm for the "half span" case (the aspect ratio is 1.9). In both cases, the forces on the hydrofoil have been measured when the hydrofoil traveled at 2 knots and 4 knots with several different yaw angles. We define the Froude number as $F_n=\frac{U_\infty}{\sqrt{gC}}$ here, where C is the hydrofoil chord length, so the above cases are equivalent to Froude numbers 0.5 and 1.0.

In the presented method, the coordinate system is fixed on the body; therefore, the inflow directs with an angle of attack (yaw angle) relative to the body when calculating the flow around a surface piercing hydrofoil with a yaw angle. Fig. 4 shows the panel arrangements on the free surface and on the hydrofoil. The panels on the hydrofoil are discretized by using a cosine spacing in both the spanwise direction and the chordwise direction. This is for the purpose of having better numerical resolutions near the free surface and at leading edge and trailing edge. The panels on the free surface are discretized by a hyperbolic tangent spacing upstream and downstream of the hydrofoil, and aligned with the panels on the hydrofoil. The panels on the hydrofoil wake are discretized with a half-cosine spacing such that panels are finer near the hydrofoil trailing edge.

We first examine the convergence of

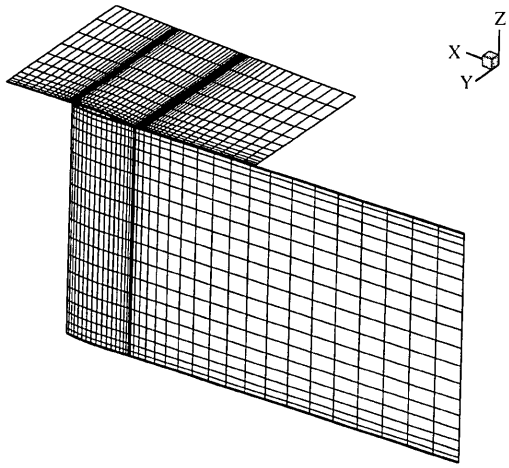

Fig. 4 Panel arrangements on the free surface and on the hydrofoil in the presented method

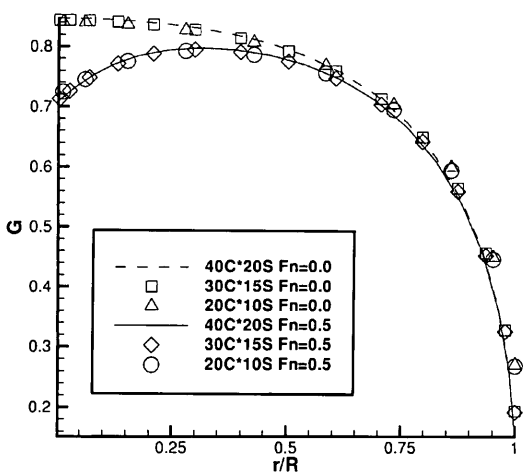

Fig. 5 Calculated circulation distributions on the hydrofoil for F_n=0 and F_n=0.5 by using different number of panels. C represents number of panels in the chordwise direction, and S represents number of panels in the spanwise direction

computational results. Fig. 5 shows the calculated circulation distributions by using different numbers of panels. In this figure, the non-dimensional circulation, G, is defined as $\frac{\Gamma}{2\pi R U_\infty}$, where Γ is the circulation strength, and R is the length of hydrofoil span. The solutions at both Froude numbers, 0.0 and 0.5, are shown in Fig. 5, and the results of both cases are convergent. Note that the zero Froude number solutions are equivalent to the double body solutions. We then investigate the lifting effect and the Kutta condition. Fig. 6 shows the wave patterns calculated by the presented method and by a source only velocity based method previously mentioned (no Kutta condition imposed), and the difference between two calculations is obvious. It is more interesting to investigate the detail flow near the trailing edge of these two computations, and Fig. 7 shows the velocities

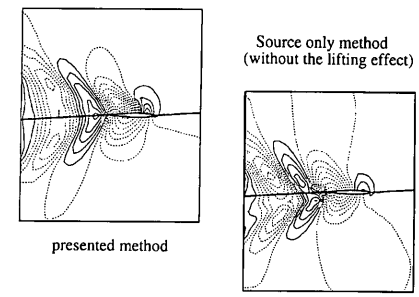

Fig. 6 Comparison of the calculated wave pattern of the "full span" hydrofoil between the presented method and a source only, velocity based method. The froude number is 0.5, and the yaw angle is 4 degrees

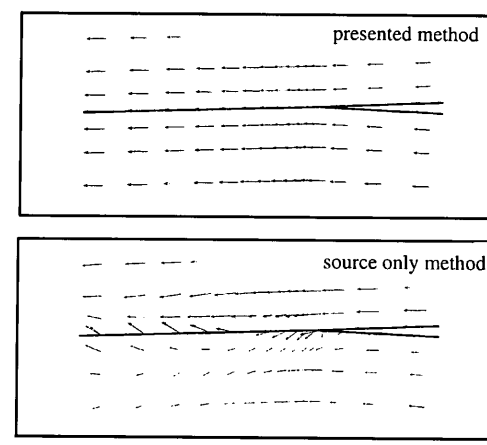

Fig. 7 Comparison of the calculated velocities near the hydrofoil trailing edge of the "full span" hydrofoil between the presented method and a source only, velocity based method. The Froude number is 0.5, and the yaw angle is 4 degrees

calculated by these two conditions. Apparently, imposing the Kutta condition makes the flow smooth near the trailing edge as one has expected.

We will then compare the calculated forces with the measured forces on the hydrofoil. Figs. 8 and 9 show the comparisons of the lift coefficients between the computational results and experimental data at two different Froude numbers for the "full span" case (aspect ratio 3.4). For both Froude numbers, computational results fail to predict the lift coefficients at 8 degrees of yaw angle, however, the comparisons of the computational results and the experimental data are good at smaller yaw angles. Figs. 10 and 11 show the comparisons of the lift coefficients between the computational results and experimental data at two different Froude numbers for the "half span" case (aspect ratio 1.9). The computational results agree well with the experimental data even at 8 degrees of yaw angle, and the comparison is especially good for Froude number 1.0. In general, the above comparisons show that the presented method can predict the

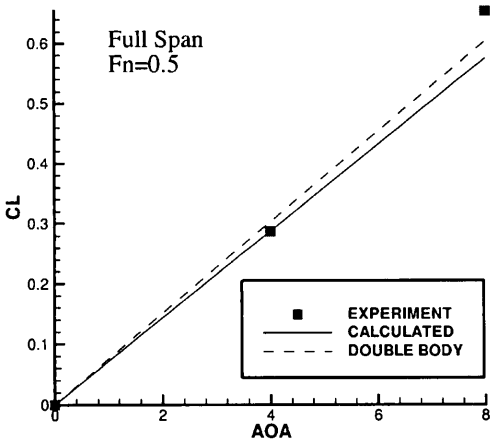

Fig. 8 Comparison of the computational lift coefficients and experimental data at Froude numbers 0.5 for the "full span" case

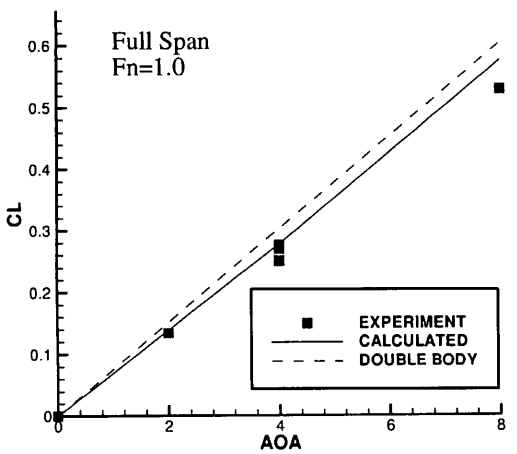

Fig. 9 Comparison of the computational lift coefficients and experimental data at Froude number 1.0 for the "full span" case

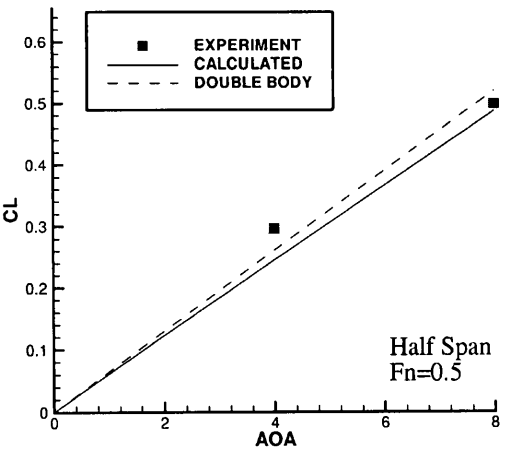

Fig. 10 Comparison of the computational lift coefficients and experimental data at Froude numbers 0.5 for the "half span" case

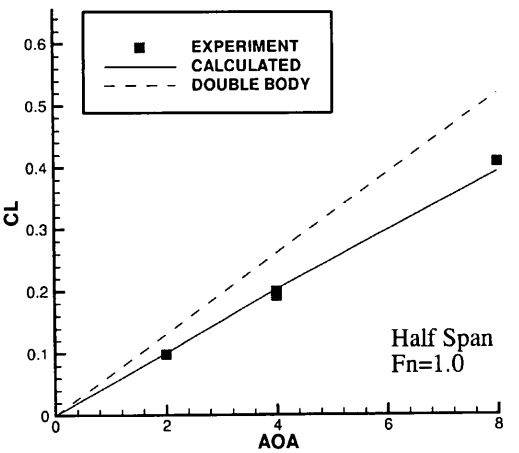

Fig. 11 Comparison of the computational lift coefficients and experimental data at Froude number 1.0 for the "half span" case

forces on a surface piercing hydrofoil reasonably accurately.

V. CONCLUSIONS

The advantages of the presented method are that, first, it is easy to implement the Kutta condition when the lifting effect is considered, and the formulation used is less complicated than research done previously. Secondly, by using a mixed boundary element method and solving the body problem and the free surface problem separately, the resulting matrices for both problems can be solved by an iterative matrix solver. Therefore, the computational time has been dramatically reduced.

In this paper, computational results for free surface flow around both non-lifting bodies and lifting bodies have been demonstrated. The comparisons between the presented method and a source only method show that results from the presented method are very close to the latter method for non-lifting bodies, and the results of the presented method are more accurate for lifting bodies because they impose the Kutta condition. The computational results have also shown reasonable agreement with the experimental data for both non-lifting bodies and lifting bodies.

The multi-zone boundary element method concept can also be applied to the presented method by appropriately dividing the body into several zones. Therefore, the analysis of flow around a catamaran, a trimaran, or a SWATH should be possible by using the presented method.

REFERENCES

1. Beaver, W.E., 1991, Pact Surface Piercing Foil

Experiments - Experiment Description and Force Data, Technical Report DTRC/SHD-1358-01, David Taylor Research Center.
2. Dawson, C.W., 1977, A Practical Computer Method for Solving Ship Wave Problems, In *Proceedings of the Second International Conference on Numerical Ship Hydrodynamics.*
3. Hess, J.L., 1972, Calculation of Potential Flow about Arbitrary Three-dimensional Lifting Bodies, Technical Report MDC J5679-01, McDonnell Douglas.
4. Hess, J.L., and Smith A.M.O., 1964, "Calculation of Nonlifting Potential Flow about Arbitrary Three Dimensional Bodies," *Journal of Ship Research*, Vol. 8, No. 2.
5. Hsin, C.-Y., 1990, *Development and Analysis of Panel Method for Propellers in Unsteady Flow*, PhD thesis, Department of Ocean Engineering, MIT.
6. Hsin, C.-Y., Kerwin, J.E., and Kinnas, S.A., 1991, "A Panel Method for the Analysis of the Flow Around Highly Skewed Propellers," In *Proceedings of the Propellers/Shafting '91 SYmposium*, Virginia Beach, VA, SNAME.
7. Kajitani, H., 1987, A Wandering in Some Resistance Components and Flow, *Ship Techn. Res.*, 34/4.
8. Kerwin, J.E., KInnas, S.A., Lee, J.-T., and Shih, W.-Z., 1987, A Surface Panel Method for The Hydrodynamic Analysis of Ducted Propellers, *Trans. SNAME*, 95.
9. Kim, Y.H., and Jenkins, D., 1981, Trim and Sinkage Effects on Wave Resistance with Series 60, c_b=0.6. Technical Report DTRC/SPD-1013-011, David Takyo Research Center.
10. Lu, C.-Y., and Chou, S.-K., 1994, "A Computational Method for Calculating Ship Wave Resistance," In *Proceedings of CFD Workshop*, volume Vol. 98, Tokyo, Japan.
11. Maniar, H., Newman, J.N., and Xu, H., 1990, "Free-surface Effects on a Yawed Surface-piercing Plate," In *Proceedings of the Enghteenth Symposium on Naval Hydrodynamics*, Ann Arbor, Michigan.
12. Morino, L., and Kuo, C.-C., 1974, "Subsonic Potential Aerodynamic for Complex Configurations: A General Theory," *AIAA Journal*, Vol. 12, No. 2, pp. 191-197.
13. Xia, F., 1986, Calculation of Lifting Potential Flow with a Free Surface, Technical Report 2912-2, SSPA.
14. Xu, H., 1991, "Potential Flow Solution for a Yawed Surface-piercing Plate," *Journal of Fluid Mechanics*, Vol. 226.

Discussions of this paper may appear in the discussion section of a future issue. All discussions should be submitted to the Editor-in-Chief.

Manuscript Received: Dec. 08, 1999
Revision Received: Jan. 19, 2000
and Accepted: Feb. 18, 2000

應用混合式邊界元素法進行升力體及非升力體於自由液面中之流場計算

辛敬業[1] 周顯光[2]

[1] 國立台灣海洋大學系統工程暨造船學系
[2] 聯合船舶設計發展中心

摘 要

本文的主要目的在於介紹一混合應用以速度爲基礎與以速度勢爲基礎的邊界元素法，提供一計算興波阻力的新途徑。此邊界元素法可計算非升力體的興波阻力，並可應用庫塔條件而計算升力體的興波阻力，其方法爲在船體上應用以速度勢爲基礎的邊界元素法，再將解答轉換爲自由液面問題中的"入流項"，在計算自由表面時，則採以速度爲基準的邊界元素法且採取Dawson處理自由液面問題的方法。在此方法的架構下，矩陣可以迭代矩陣解法來解，大量縮短了計算時間。本文顯示本方法與傳統Dawson方法計算結果的差異，並進行升力體與非升力體興波阻力計算結果與實驗資料的比較。

關鍵字：邊界元素法，自由液面，興波阻力，庫塔條件。